A Numerical Procedure for the Optimization of IGBT Module Packaging

Hua Lu†, Pushparajah Rajaguru and Chris Bailey
Department of Mathematical Sciences, University of Greenwich,
London, UK
†Email: H.Lu@gre,ac.uk

***Abstract*—A numerical solution procedure for optimizing the thermal-mechanical reliability of an IGBT module has been described in this paper. The procedure is robust and it can handle both discrete and continuous decision variables in the design of IGBT packaging. An example has been given to demonstrate its application. The objective functions in this example are the accumulated plastic work density in solder joints of a simplified IGBT module that is subject to cyclic temperature cycling and the maximum junction temperature when the model is subject to a constant thermal loading. The thickness of the chip mount-down solder, thickness of the substrate solder joint, and the location of the chip are used as continuous decision variables. The material selection for the baseplate is treated as a discrete variable. The objective function values are calculated using Finite Element Analysis method.**

Keywords—IGBT; Multi-objective Optimization; Finite Element;

I. INTRODUCTION

Power electronics systems are found in numerous industrial and domestic applications and their design and manufacturing are key to the success of energy generation, conversion, distribution. At the heart of power electronics systems are semiconductor devices such IGBT modules which are crucial in defining the performance and reliability of power electronics systems [1].

Fig. 1 shows that the structure of an IGBT module which consists of silicon chip, chip solder, DBC copper, ceramic substrate, DBC copper, substrate solder, baseplate, wirebonds and busbars. This highly inhomogeneous structure is susceptible to thermal mechanical failures that are caused by thermal mechanical fatigue near material interfaces. One of the important issue for packaging designers and manufacturers to minimize the risk of these failures.

As a potentially cost-effective design method, virtual prototyping has been widely used in the industry. It can speed up the design and testing process and to achieve designs with optimal functional performance and reliability. The software tools that are used for virtual prototyping can be general software packages but they could also be specialized software tools such as the one that has been proposed by Evan et al [2]. The advantages of the latter over general purpose software tools for design optimization are that it can be simpler to develop, quicker to learn and more efficient.

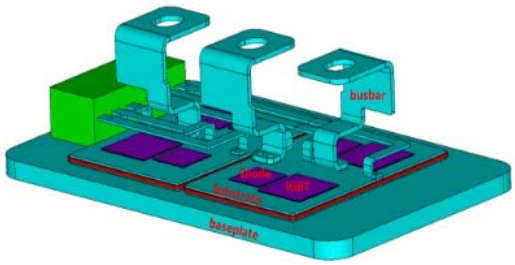

Fig. 1. The structure of an IGBT module which contains 4 IGBT-diode pairs. The wirebonds are not shown in the drawing.

In any virtual design tool, one of the important part is a numerical optimization algorithm that can be used to find the optimal design automatically. Typical engineering designs are affected by many parameters and there could also be more than one objective function. This means that design engineers must deal with multi-objective-optimization (MOO) problems in multi-dimensional design spaces. Furthermore, the decision variables can be continuous discrete. In this work, the aim is to develop a robust MOO procedure that is capable of solving IGBT design problems that are multi-objective and have both continuous and discrete variables. The method is based on particle-swarm optimization (PSO) and therefore it will be called a multi-objective particle swarm optimization (MOPSO) method.

II. METHODOLOGY

For a problem with l continuous decision variables (DVs), m discrete DVs, n objective functions (OBJs), p inequality constraints and q equality constraints, the optimization problem can be expressed as following.

$$\min\{F_1(X), F_2(X), \dots F_n(X)\} \quad (1)$$

where $X = (x_1, \dots x_l, x_{l+1}, x_{l+m})$.

$$x_i^{min} \le x_i \le x_i^{max}, 1 \le i \le l+m \quad (2)$$

$$G_j(X) \le 0, \quad 1 \le j \le p \quad (3)$$

$$H_k = 0, \quad 1 \le k \le q, \quad (4)$$

where x_i are decision variables, X is the DV variable vector, F_i(X) are objective functions, G_j and H_k are state variables for constraints, x_i^{min} and x_i^{max} are the lower and higher bounds of the i-th DV.

2018 19th International Conference on Electronic Packaging Technology
978-1-5386-6386-8/18/$31.00 ©2018 IEEE

A. PSO and MOPSO

PSO is a metaheuristic method for solving optimization problems [3,4]. It doesn't use OBJ functions' gradient which may make it slower to converge than gradient based methods but it is simple to implement and suitable for problems in which gradients are difficult or impossible to come by. For one objective optimization, PSO can be described as follows.

Randomly select N initial candidate solutions in the design space. These solutions are called "particles", and then these solutions evolve for required number of iterations and the optimal solution is obtained at the end of the process.

The position of the i-th particle in the design space is represented by a vector $X_i = (x_1, x_2 \dots x_l)$ where l is the dimension of the design space (i.e. the number of DVs). At the t-th iteration, this vector is written as $X_i(t)$. Assuming that the i-th particle's best (local) solution so far at the t-th iteration is P_i, and the best (global) solution of all particles is G, a velocity vector for the i-th particle can be calculated using Eq. 5.

$$v_i(t+1) = v_i(t) + C_1 r_1\big(P_i - X_i(t)\big) + C_1 r_2\big(G - X_i(t)\big) \quad (5)$$

where C_1 and C_2 are constant parameters and r_1 and r_2 are random numbers with values between 0 and 1. As it is suggested in [3], it is assumed that $C_1 = C_2 = 2$ in this work. At the next iteration, the particle's location is updated using Eq. 7 for both the continuous and discrete DVs but for the latter, the values are rounded to the nearest integers.

$$X_i(t+1) = X_i(t) + v_i(t+1) \quad (6)$$

In MOMOO problems, there is no single 'best solution', global or local and the algorithm needs modification. A local set L_i is used to store N_L (which is a predefined size of the set) solutions that are selected from the i-th particle's past solutions. A solution in L_i is not dominated by any others in the set which means that other solutions are not better for all the OBJs. From the solutions in local sets of all the particles, a global set G with N_g solutions are created by using a Pareto filter [5] and N_g is a predefined global set size. L_i and G are updated at each iteration and new members may be added and the sizes of the L_i and G are controlled using crowding distance [6]. If the number of solutions in a set exceeds the size of the set, only the members with the longest crowding distances are kept.

To update the i-th particle's velocity, a local leader is selected randomly from L_i, and a global leader is selected from solutions in G and the selected global leader has either the longest or the shortest Euclean distance to particle i [7]. In this work, the velocity also includes a diversity preservation term for both continuous and discrete DVs [7]. For continuous and discrete DVs the terms are described in [7,8]. At the end of the iterative process, G contains the final solutions that form the Pareto front.

B. Finite Element Analysis, DOE and Surrogate Models

In solving an optimization problem, OBJ functions can be simple analytical expressions but for engineering design problems their evaluation has to rely on experiments or computer simulation. In this work, FEA is used to evaluate OBJs in the design optimization of IGBTs. Optimization may need large number of OBJ and other function evaluations and FEA simulation itself is often time consuming. This makes optimization computationally expensive. In this work, design of experiment (DOE) and FEA are used to produce simple surrogate models, which are then used for OBJ function evaluation.

III. IGBT DESIGN OPTIMIZATION

One of the major IGBT failure mechanisms is the (substrate or chip) solder joint fatigue that is caused by temperature fluctuation in operation or during qualification tests. When the temperature change is relatively slow, as in temperature cycling tests, the reliability of the solder joints can be predicted using plastic strain or plastic work density W_p in the solder layers for each loading cycle. When an IGBT is in operation or in some power cycling tests, the chips may experience rapid and often random changes in loading and in this situation, there isn't enough time for heat energy to disperse and the raised junction temperature could affect the reliability of IGBTs. The junction temperature in this situation is to a great extent depend on the thermal resistance. Therefore both the thermal resistance and the maximum junction temperature T_{max} are good reliability metrics for predicting the reliability of IGBT packages in operation or in power cycling tests [9]. In this work, W_p and T_{max} are assumed to be the OBJs that will be minimized for optimal IGBT designs using MOO methods.

A. FEA model

Fig. 2 shows the structure of the IGBT that is studied. In Table I, the nominal dimensions of the structure are listed.

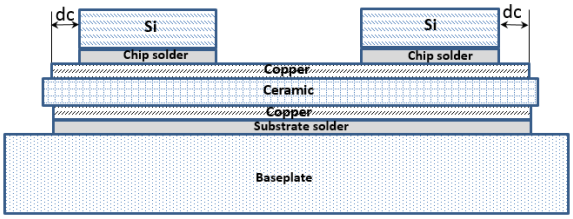

Fig. 2. IGBT structure. d_c is a parameter to describe the location of the IGBT die relative to the substrate.

TABLE I. TYPICAL DIMENSIONS OF THE IGBT STACK. THE UNITS ARE IN mm.

Chip	5x5x0.3
chip solder	5x5x0.1
DBC Cu	30x30x0.3
Ceramic	32x32x1.0
Substrate solder	30x30x0.3
Baseplate	40x40x3

To save computational time, 2D FEA is used to evaluate OBJs for given designs and loading conditions. Fig. 3 shows the model and part of the FEA mesh.

Apart from the solder alloy, the materials in the model are linear-elastic. For the solder alloy, Eq. 8, which is a creep strain rate model, is used to represent its nonlinear property. The property values are listed in Table II. The unit for the Young's modulus E, coefficient of thermal expansion α and the thermal conductivity k are GPa, 1/K and W/(mK) respectively. In the

table, ν is the Poisson's ratio which is dimensionless. In Table II, A=54.05-0.193(T-273.15) and B=21.85+0.02039(T-273). The baseplate is assumed to be Cu, AlSic and a fictitious baseplate material (FBM) whose properties are the average of Cu and AlSiC.

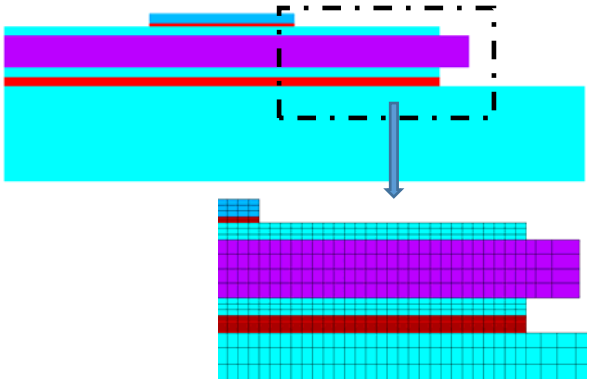

Fig. 3. 2D FEA model of the IGBT. Top: CAD drawing showing the ½ 2D model. Bottom: close up of the mesh around the edge of the substrate.

Eq. 7 shows the strain rate for the solder alloy.

$$\dot{\varepsilon}_{cr} = A \cdot sinh^{n}(\eta\sigma_e)\exp(-Q/RT) \qquad (7)$$

where $\dot{\varepsilon}_{cr}$ is the creep strain rate, σ_e is the effective stress, R is the universal gas constant, T is temperature in K, A, η and Q are material constants that are listed in Table III.

TABLE II. THERMAL AND MECHANICAL MATERIAL PROPERTIES.

	E	ν	α (10^{-6})	k
Cu (DBC and baseplate)	103	0.3	17	385
AlN	330	0.24	5.6	150
AlSiC (baseplate)	255	0.24	6.3	180
Si(chip)	131	0.3	2.8	150
Sn3.5Ag (solder)	A	0.4	B	60
FBM	179	0.27	11.7	283

TABLE III. VISCO-PLASTIC MODEL PARAMETERS FOR SN3.5AG SOLDER [10]

A (s^{-1})	n	η (1/MPa)	Q/R(K)
$9x10^5$	5.5	0.06527	8690

In the stress analysis, a cyclic temperature loading is applied. The maximum and minimum temperatures are -40 ºC and 125 ºC respectively, and the dwell times and ramp times are all 900 s. Fig. 4 shows a typical plastic work density distribution. The OBJ W_p is the mean of the element values at the edge of solder layers over a cycle.

In the thermal analysis, steady state temperature distribution is predicted and 100W of power is applied to the top of the chip, a convective boundary condition is applied at the bottom of the baseplate. The heat transfer coefficient and the fluid temperature are assumed to be 30000 W/(m²•K) and 293K respectively. Fig. 5 shows a typical temperature distribution. The OBJ T_{max} is simply the maximum junction temperature. *ANSYS® Academic Research Mechanical, Release 17.2* has bee used for FEA analysis in this work.

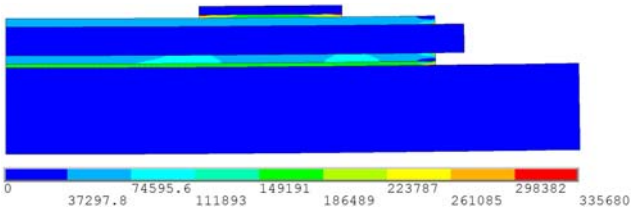

Fig. 4. Plastic work density distribution at t=3600s. The unit is J/m³. The chip solder thickness, substrate solder thickness, and dc are 0.11 mm, 0.14 mm and 3.25 mm respectively. and 3 respectively. The baseplate material is AlSiC.

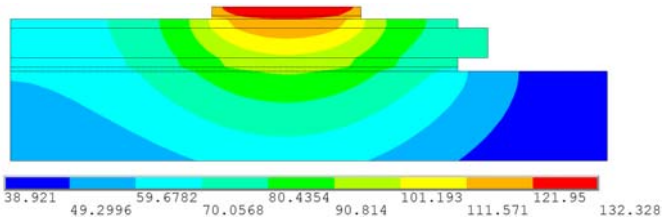

Fig. 5. Temperature distribution. The chip solder thickness, substrate solder thickness, and dc are 0.11 mm, 0.14 mm and 3.25 mm respectively. and 3 respectively. The baseplate material is AlSiC.

B. DOE and Surrogate Models

The chip solder thickness t_c, the substrate solder thickness t_s, chip location d_c and the baseplate material type M_b are chosen as the DVs and the design space is defined in Table IV. The discrete parameter M_b has integer values of 1, 2 and 3 and it represents Cu, FBM and AlSiC baseplate materials.

A full factorial composite DOE method has been used to select designs to represent the whole design space. The number of designs is 2^n+2n+1 where n is the number of DVs. For n=4, the 25 designs are listed in Table V for scaled DVs.

TABLE IV. DECISION VARIABLES.

	t_c(mm)	t_s(mm)	d_c(mm)	M_b
min	0.06	0.08	1	1
max	0.16	0.2	7	3

TABLE V. FULL FACTORIAL COMPOSITE DESIGNS FOR FOUR DVS.

t_c	1	1	1	1	1	1	1	1	-1	-1	-1	-1	-1	-1	-1	-1	1	-1	0	0	0	0	0	0	0
t_s	1	1	1	1	-1	-1	-1	-1	1	1	1	1	-1	-1	-1	-1	0	0	1	-1	0	0	0	0	0
d_c	1	1	-1	-1	1	1	-1	-1	1	1	-1	-1	1	1	-1	-1	0	0	0	0	1	-1	0	0	0
M_b	1	-1	1	-1	1	-1	1	-1	1	-1	1	-1	1	-1	1	-1	0	0	0	0	0	0	1	-1	0

Two case studies have been carried out, both are two-objective problems. In case 1, the two OBJs are the plastic work density in the chip solder W_c and the junction temperature T_{max}, and in case 2 they are the substrate solder plastic work density W_s and T_{max}. The values of these OBJs are obtained using FEA for all the designs in Table V. Second order polynomials are then

fitted to the OBJ values using stepwise regression method [visualdoc] to produce surrogate models of the OBJs. This method may not results in full quadratic models because the parameters for some terms are negligible. In Table VI, the polynomial cofficients for OBJ surrogate models are listed.

TABLE VI. COEFFICIENTS OF THE SECOND ORDER POLYNONIAL RESPONSE SURFACE FOR NON-SCALED DECISION VARIABLES.

T_{max}	
terms	coefficients
Constant	116.5
t_c	3.2
t_s	2.0
d_c	-0.9
$t_s d_c$	-0.375
d_c^2	4.194

W_s		
terms	coefficients	
Constant	2.0	0.0881
t_s	-7.41	1.54
M_b	-0.967	0.081
$t_s M_b$	1.37	0.145
t_s^2	9.58	5.39
M_b^2	0.156	0.0194

W_c		
terms	coefficients	
Constant	0.286	0.00862
t_c	-1.789	0.143
d_c	-0.00440	0.0009
M_b	0.0953	0.00237
$t_c d_c$	0.0158	0.00577
$t_c M_b$	-0.46	0.0173
$d_c M_b$	0.000625	0.000289
t_c^2	7.737	0.617

C. Results and discussions

In MOO, the optimal solutions are described by the Pareto Front which consists of a number of non-dominated solutions. Any solution on the Pareto Front can't be improved in one OBJ without causing deterioration in another OBJ.

Fig. 6 shows the distribution of 2000 random feasible solutions for the case 2 where W_s and T_{max} are the OBJs. It shows the feasible solutions form clusters that correspond to the discrete variable M_b. In this simple two-objective problem, the Pareto Fronts can be identified as part of the outlines of the solutions. It can be seen in the figure that none of the solutions for M_b=3 could be on the Pareto optimal solution because both OBJ values for M_b=3 are worse than some of the solutions in for M_b=2, i.e. all solutions for M_b=3 are dominated.

To obtain the optimal solution, a population size of 50, local and global set size of 10 and 30 respectively. Fig. 7 shows the Pareto front at iterations 1, 4 and 40. Fig. 8 shows the Pareto front for cases 1&2 after 100 iterations. The results show that the convergence to the final solution is rapid and the designs are distributed evenly.

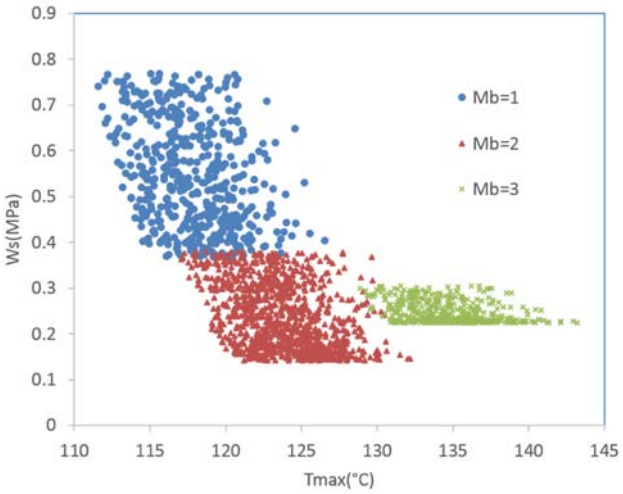

Fig. 6. Distribution of 2000 random solutions in the W_s-T_{max} case.

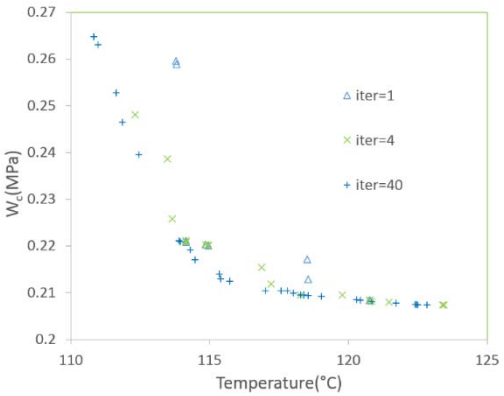

Fig. 7. Pareto front at iterations 1, 4 and 40 for the case 1.

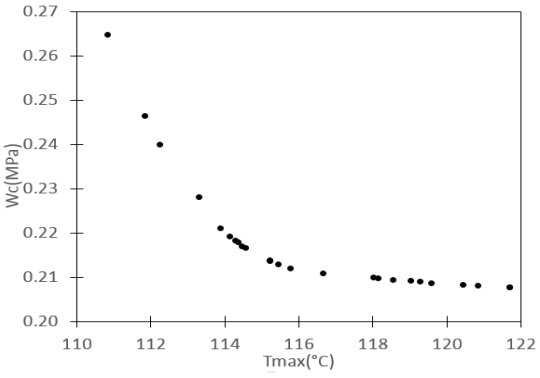

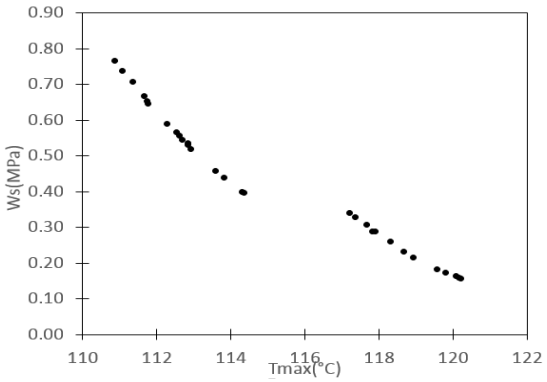

Fig. 8. Pareto front for case 1 (top) and 2 (bottom).

IV. CONCLUSIONS

A MOPSO algorithm has been described in the paper. It has been demonstrated that it can be used for the MOO of IGBT in packaging design for optimal reliability. The algorithm is simple to implement and robust. Further work will be carried out to compare its efficiency with other optimization methods, to investigate the stopping criteria and the optimal population, local and global set sizes.

ACKNOWLEDGMENT

The authors would like to acknowledge the financial support from EPSRC UK grants EP/K034804/1 and EP/R004390/1.

REFERENCES

[1] S. Yang, A. Bryant, P. Mawby, D. Xiang, L. Ran and P. Tavner, "An Industry-Based Survey of Reliability in Power Electronic Converters," in *IEEE Transactions on Industry Applications*, vol. 47, no. 3, 2011 pp. 1441-1451

[2] P. L. Evans, A. Castellazzi and C. M. Johnson, "Design Tools for Rapid Multidomain Virtual Prototyping of Power Electronic Systems," in IEEE Transactions on Power Electronics, vol. 31, no. 3, 2016, pp. 2443-2455

[3] J. Kennedy and R. Eberhart, "Particle swarm optimization," *Neural Networks, 1995. Proceedings., IEEE International Conference on*, Perth, WA, 1995, pp. 1942-1948 vol.4.

[4] Y. Shi, R.C. Eberhart, "A modified particle swarm optimizer". Proceedings of IEEE International Conference on Evolutionary Computation. 1998, pp. 69–73

[5] A. Messac, A. Ismail-Yahaya, C.A. Mattson, "The normalized normal constraint method for generating the Pareto frontier", Structural and Multidisciplinary Optimization, July 2003, Vol. 25, Issue 2, pp 86-98

[6] K. Deb, A. Pratap, S. Agarwal and T. Meyarivan, "A fast and elitist multiobjective genetic algorithm: NSGA-II," in *IEEE Transactions on Evolutionary Computation*, vol. 6, no. 2, 2002, pp. 182-197

[7] W. Tong, S. Chowdhury, A. Messac, "A multi-objective mixed-discrete particle swarm optimization with multi-domain diversity preservation", Structural and Multidisciplinary Optimization, Volume 53, Issue 3, 2016, pp 471-488

[8] S. Chowdhury, W. Tong, A. Messac, J. Zhang, "A mixed-discrete Particle Swarm Optimization algorithm with explicit diversity-preservation", Struct Multidisc Optim. Vol. 47, Issue 3, 2013, pp 367–388

[9] B. Ji, X. Song, E. Sciberras, W. Cao, Y. Hu and V. Pickert, "Multiobjective Design Optimization of IGBT Power Modules Considering Power Cycling and Thermal Cycling," in IEEE Transactions on Power Electronics, vol. 30, no. 5, 2015, pp. 2493-2504

[10] J.H. Lau, (editor), Ball Grid Array Technology, McGraw-Hill, 1995, pp.396